

Title	Fabrication of spintronics device by direct synthesis of single-walled carbon nanotubes from ferromagnetic electrodes
Author(s)	Mohamed, Mohd Ambri; Inami, Nobuhito; Shikoh, Eiji; Yamamoto, Yoshiyuki; Hori, Hidenobu; Fujiwara, Akihiko
Citation	Science and Technology of Advanced Materials, 9(2): 025019-1-025019-5
Issue Date	2008-07-24
Type	Journal Article
Text version	publisher
URL	<a href="http://hdl.handle.net/10119/4735">http://hdl.handle.net/10119/4735</a>
Rights	Copyright (c) 2008 National Institute for Materials Science. M. A. Mohamed, N. Inami, E. Shikoh, Y. Yamamoto, H. Hori, and A. Fujiwara, Science and Technology of Advanced Materials, 9(2), 2008, 025019. <a href="http://stacks.iop.org/STAM/9/025019">http://stacks.iop.org/STAM/9/025019</a>
Description	

# Fabrication of spintronics device by direct synthesis of single-walled carbon nanotubes from ferromagnetic electrodes

Mohd Ambri Mohamed, Nobuhito Inami, Eiji Shikoh,  
Yoshiyuki Yamamoto, Hidenobu Hori and Akihiko Fujiwara

School of Materials Science, Japan Advanced Institute of Science and Technology (JAIST),  
1-1 Asahidai, Nomi, Ishikawa 923-1292, Japan

E-mail: [ambri@jaist.ac.jp](mailto:ambri@jaist.ac.jp)

Received 25 December 2007

Accepted for publication 20 April 2008

Published 24 July 2008

Online at [stacks.iop.org/STAM/9/025019](http://stacks.iop.org/STAM/9/025019)

## Abstract

We describe an alternative method for realizing a carbon nanotube spin field-effect transistor device by the direct synthesis of single-walled carbon nanotubes (SWNTs) on substrates by alcohol catalytic chemical vapor deposition. We observed hysteretic magnetoresistance (MR) at low temperatures due to spin-dependent transport. In these devices, the maximum ratio in resistance variation of MR was found to be 1.8%.

Keywords: single-walled carbon nanotubes (SWNTs), alcohol catalytic chemical vapor deposition (ACCVD), direct synthesis, magnetoresistance (MR), spintronics device

(Some figures in this article are in colour only in the electronic version)

## 1. Introduction

Carbon nanotubes (CNTs) are considered to be a potential material for spin electronics device applications. They exhibit a long electron mean free path [1, 2] and weak spin-orbit coupling; thus, the spin diffusion length is expected to be extremely large [3]. Spin-dependent transport in carbon nanotubes was originally demonstrated in multi-walled carbon nanotubes (MWNTs) with ferromagnetic contacts [4]. For spin electronics application, however, single-walled carbon nanotubes (SWNTs) have many advantages over MWNTs. A greater spin diffusion length and a well-defined electron band structure can be expected in SWNTs. In this paper, we report the direct fabrication of SWNTs on patterned substrates by alcohol catalytic chemical vapor deposition (ACCVD) to form spin field-effect transistor (FET) devices, and we discuss their magnetoresistance (MR) behavior. We adopt a Co catalyst for SWNT growth, which also acts as a ferromagnetic contact, to inject a spin-polarized current inside the nanotube in order to observe any MR effects.

## 2. Experimental details

### 2.1. Device fabrication and catalyst preparation

In the direct synthesis of SWNTs in FETs, a Mo/Co bilayer was used both as the catalyst for the SWNT growth and as ferromagnetic electrodes. The FETs fabricated in this study had the back-gate configuration, as shown in figure 1(a). A heavily doped n-type silicon wafer with a 400-nm-thick thermally oxidized SiO<sub>2</sub> layer on the surface was used as the substrate. The SiO<sub>2</sub> layer and the doped silicon layer of the wafer were used as the gate insulator and gate electrode, respectively. The source and drain electrodes were patterned on the insulating SiO<sub>2</sub> layer by photolithography. The channel length  $L$  was fixed at 5  $\mu\text{m}$  and the channel widths  $W$  were designed to be 250 and 500  $\mu\text{m}$ , as shown in figure 1(b). Mo was first deposited on the substrate using an electron-beam evaporation system to a thickness of 100 nm. After the deposition of Mo, the substrate was subsequently tilted 8° for the following deposition of the Co catalyst, as illustrated in figure 1(c). The Co catalyst was then deposited using the electron-beam evaporation system to a nominal thickness of

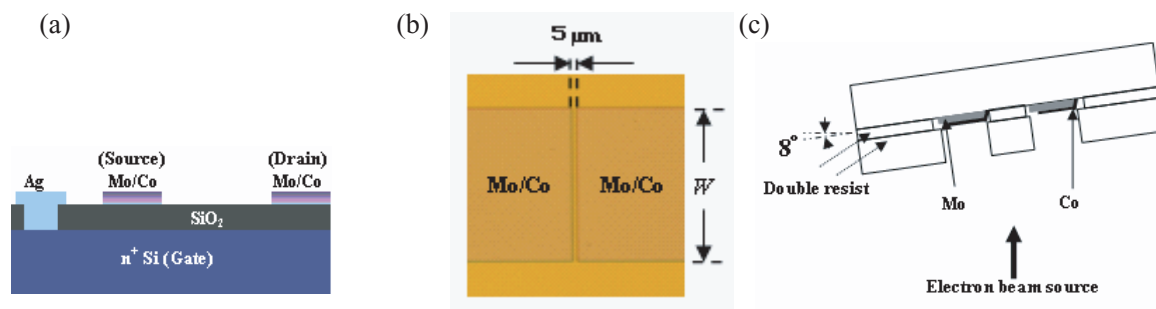


**Figure 1.** (a) Schematic drawing of device structure, (b) optical microscope image of Mo/Co electrodes on the  $n^+$ -Si/SiO<sub>2</sub> substrate, (c) schematic drawing of setup for the angled deposition of Co.

1 nm. The tilted deposition technique shown in figure 1(c) was also employed to deposit Co on the side of the Mo to enhance the growth of SWNTs along the channel.

## 2.2. SWNT synthesis by ACCVD

SWNTs were synthesized on the Co catalyst by ACCVD with ethanol as a feed gas. After the catalyst was deposited, the substrate was subsequently transferred to the CVD reactor. The reactor was evacuated by a rotary pump to a pressure of 1 Pa, while the furnace was heated to 900 °C at a position 30 cm away from the substrate. A mixed gas flow of Ar/H<sub>2</sub> (3% H<sub>2</sub>) was used to purge the CVD reactor at an internal pressure of 200 Pa. When the furnace temperature reached the synthesis temperature, the furnace was immediately transferred to the substrate position for rapid heating [5]. The Ar/H<sub>2</sub> gas flow was then terminated and ethanol was immediately fed into the reactor at a flow rate of 6.0 litre/min<sup>-1</sup> to start the decomposition of ethanol. The catalytic reaction of ethanol continued for 30 min. During the reaction, the internal pressure of the CVD reactor was 3.2 kPa. After the synthesis, the furnace was removed from the substrate position and the ethanol gas flow was stopped. The substrate was left to cool naturally. The quartz tube used for this reactor was 1200 mm in length and 26 mm in inner diameter. The SWNTs grown on the substrate were characterized by scanning electron microscopy (SEM, Hitachi S4100), atomic force microscopy (AFM, Seiko Instruments) and Raman spectroscopy with a laser excitation energy of 632.8 nm (Tokyo Instruments, Nanofinder 30).

## 2.3. Electric conductivity and spin transport

The resistance between the source and drain electrodes was measured by the two-terminal method using a resistance bridge (Picowatt AVS-47) with an excitation voltage of 3 mV and a frequency of 15 Hz. For reference, the resistance of patterned electrodes on substrates before ACCVD was also measured to exclude the extrinsic effects of the current flow. The devices were mounted in a continuous-flow helium cryostat. The MR measurements were performed by setting the cryostat in an electromagnet system. The magnetic field was applied parallel to the tube axis in the plane of the substrate [6]. Measurements were carried out at room temperature and at 4.5 K. The field was swept from 0 to 2000 Oe, then back to -2000 Oe, and measurement stopped

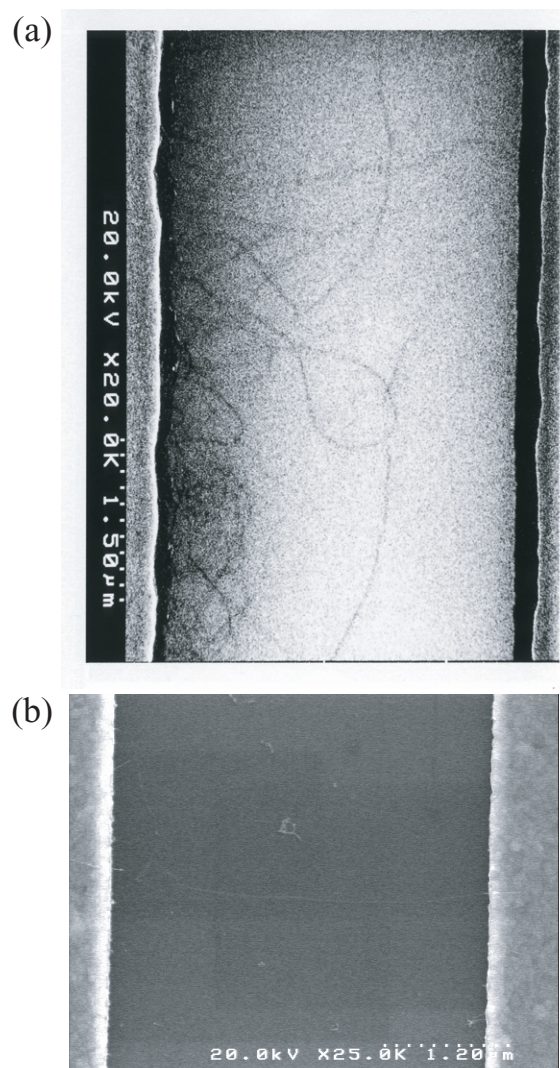


**Figure 2.** SEM image around and between a pair of Mo/Co electrodes, (b) SEM image of the area between the electrodes showing contacts between nanotubes and Co nanoparticles.

at 2000 Oe. As a control experiment, we also measured the MR effect in one of the electrodes.

## 3. Results and discussion

Figure 2(a) shows an SEM image around and between a pair of Mo/Co electrodes after ACCVD. The left and right edges correspond to the Mo/Co electrodes. Fine structures between

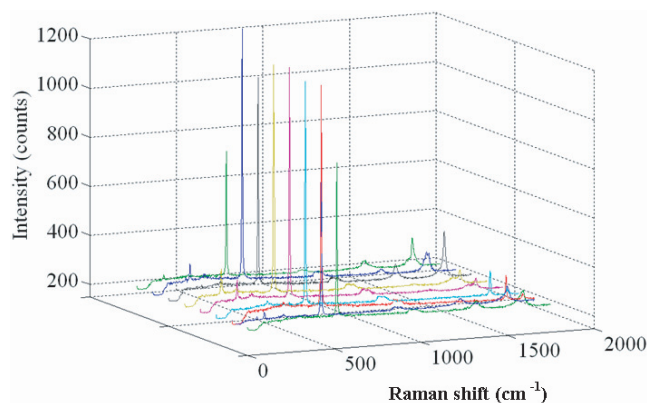
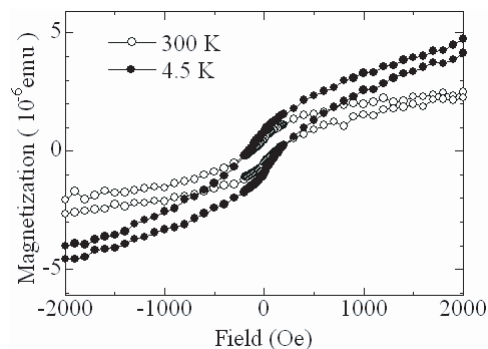


**Figure 3.** Raman spectra obtained at intervals of 500 nm around the boundary of the electrode.

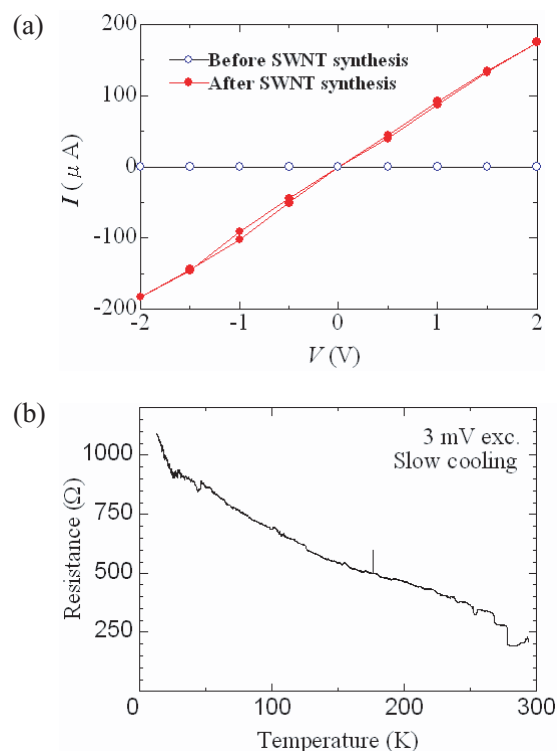
the electrodes were observed, some of which successfully bridged the electrodes. These fine structures were confirmed to be SWNTs, as discussed below. SWNTs grew from Co nanoparticles that formed at high temperatures during the synthesis. The Co nanoparticle size distribution was estimated by Gaussian fitting to be  $6.6 \pm 3.3$  nm. It was confirmed that almost 500 bundles consisting of 1–10 SWNTs bridge the electrodes. The nanotubes between the electrodes were successfully grown only for the device made by the angled deposition technique, as shown in figure 1(c). Figure 2(b) shows another SEM image of a different area between the electrodes used to clarify the nature of the SWNT/Co contacts. The image clearly shows that the SWNTs are in direct contact with Co nanoparticles at both electrodes. To determine the quality of the nanotubes synthesized by this method, Raman spectroscopy measurements were performed. Figure 3 shows Raman spectra obtained at constant intervals around the boundary of an electrode. The Raman spectra exhibit radial breathing mode (RBM) peaks from  $100$  to  $350$   $\text{cm}^{-1}$ , which are characteristic of SWNTs, and G-band peaks at approximately  $1590$   $\text{cm}^{-1}$ . The strong peak at approximately  $500$   $\text{cm}^{-1}$  originates from the Si substrate. Although there are some peaks appearing in the D-band region, RBM and G-band peaks are dominant, and they match those in typical Raman spectra of SWNTs. From these results, it is concluded that the SWNTs can be successfully grown to bridge the pair of Mo/Co electrodes by ACCVD, as presented in sections 2.1 and 2.2.

Figure 4 shows the magnetic properties of the device measured by a superconducting quantum interference device (SQUID), which confirmed that the magnetic properties of Co ferromagnetic components remain unchanged at room temperature and at 4.5 K. The coercive force obtained from the hysteresis curve for both temperatures is about 120 Oe. Although Co forms fine nanoparticles on bulk Mo after annealing, its macroscopic magnetic properties are unchanged.

Current  $I$  versus voltage  $V$  characteristics for the devices before and after ACCVD are shown in figure 5. A pronounced enhancement in current was observed for the devices after SWNT growth by ACCVD, whereas no current was observed in the device before ACCVD. We



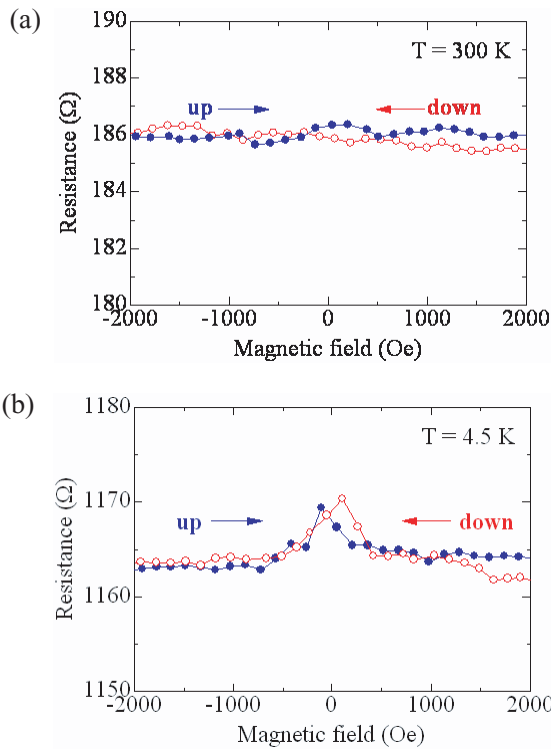
**Figure 4.** Magnetic properties of device after SWNT synthesis at 300 and 4.5 K.



**Figure 5.** (a) Current versus voltage plots for the fabricated devices before and after ACCVD, (b) temperature dependence of resistance for the device fabricated by ACCVD.

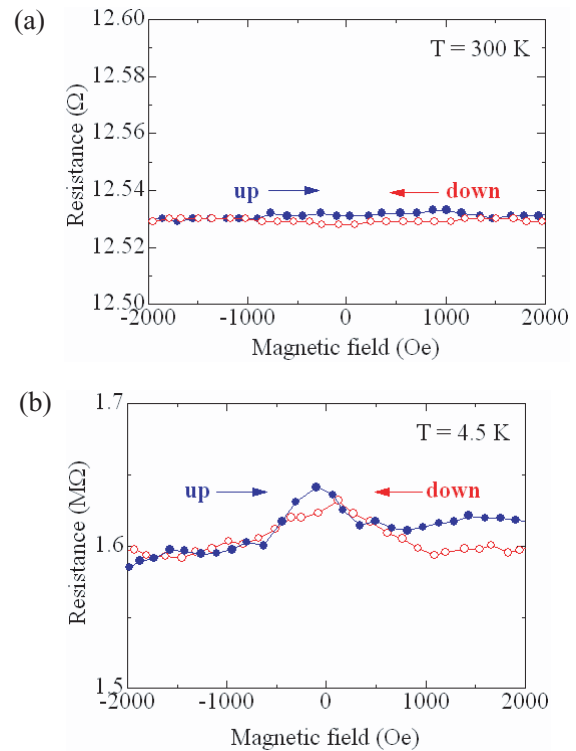
can conclude that the current flows through the SWNTs connecting the pair of electrodes. The resistance of the SWNT devices is about 10–200  $\Omega$  at room temperature. Although resistance increases with decreasing temperature, as shown in figure 5(b), it does not show activation-type temperature dependence. Therefore, the dominant current paths do not consist of semiconducting SWNTs. In agreement with this, no gate voltage dependence was observed. Note that two types of samples were synthesized by ACCVD, which exhibit either high resistance or low resistance. High-resistance samples show good FET characteristics [7]. These facts also suggest that the channels consist of metallic or semiconducting SWNTs, but not other conductive carbon materials. In this study, we mainly focused on the devices with low resistance.

Figure 6(a) shows that resistance of a device with a channel width of  $500$   $\mu\text{m}$  at 300 K is almost constant against



**Figure 6.** Magnetoresistance for the device with  $W = 500 \mu\text{m}$  at (a) 300 K and (b) 4.5 K. The closed circles (open circles) correspond to the positive (negative) sweep direction.

magnetic field at 186  $\Omega$ . However, figure 6(b) shows that resistance at 4.5 K peaks at approximately 0 Oe, and the peak varies slightly on the direction of the sweep. When the field was swept upward, a peak appeared at about  $-110$  Oe, and when it was swept downwards, a peak appeared at about 110 Oe. For the device with a channel width of  $250 \mu\text{m}$ , similar behaviour was observed to that in the device with the channel width of  $500 \mu\text{m}$ , as shown in figures 7(a) and (b). To ensure that this MR effect is not governed by the MR of Co nanoparticles on the electrodes, a control experiment was conducted. We measured the MR effect for one of the electrodes at the same temperatures. As a result, no significant change in resistance was observed. This indicates that the hysteretic MR does not originate from the Co nanoparticles themselves. Although the Co ferromagnetic component is independent of temperature, as mentioned above, MR effects were observed at a low temperature. For spin transport without spin scattering through a material connected to two ferromagnetic electrodes, the resistance is high when the ferromagnetic moments in the two electrodes are antiparallel, and low when the ferromagnetic moments are parallel [8]. The spin-valve effect observed in MWNTs [4, 9, 10] and SWNTs [9, 10] is well explained by this model. Our result in this work, however, cannot be simply explained by this model. SWNTs seem to grow from Co nanoparticles, which form from Co thin film on Mo film during ACCVD [11]. Therefore, spin-dependent transport is expected to be governed by the magnetic properties of Co nanoparticles to which the SWNTs are attached and to be strongly dependent on the size of the Co nanoparticles. Each SWNT is attached to a Co nanoparticle with a different size. Thus, it is expected that each SWNT



**Figure 7.** Magnetoresistance for the device with  $W = 250 \mu\text{m}$  at (a) 300 K and (b) 4.5 K. The closed circles (open circles) correspond to the positive (negative) sweep direction.

should show MR peaks at different field values where parallel and antiparallel magnetization configurations of the electrodes change. However, the magnetic property of an individual Co nanoparticle in contact with an SWNT cannot be determined. In this study, the average magnetic properties and MR effects of Co nanoparticles were observed. The sharp peaks of averaged MR at approximately  $\pm 110$  Oe correspond to the average coercive force measured by the SQUID. The origin of this unusual MR hysteresis still remains unclear, but the results of the MR effects are reproducible. A detailed analysis of the spin transport mechanism of these devices is to be carried out in the near future.

The ratio of MR is defined by  $\Delta R/R_0$ , where  $R_0$  is the resistance in the saturation region. At 4.5 K,  $\Delta R/R_0$  is found to be about 0.7–1.8%. This value agrees with the previous report on the MR of SWNTs [12]. To increase  $\Delta R/R_0$ , effective spin injection from the ferromagnetic electrode to the SWNTs, and spin-coherent transport in SWNTs should be realized. For spin injection, improvement in the Co/SWNT interface quality is necessary. For spin-coherent transport, the growth of high-quality SWNTs and the reduction of  $L$  between the electrodes are the most important factors. It is also interesting that the dependence of  $\Delta R/R_0$  on  $L$  can be used to clarify the spin diffusion length of SWNTs.

#### 4. Summary

We have directly synthesized SWNTs from a Co catalyst on a Mo thin film in FET devices by ACCVD. We investigated the structural properties by SEM, AFM, Raman spectroscopy,

and measured the temperature and magnetic field dependence of the magnetic and transport characteristics. Clear MR peaks with  $\Delta R/R_0$  of up to 1.8% were observed at 4.5 K. This result can be attributed to the spin-dependent transport in SWNT FETs fabricated by direct synthesis.

### Acknowledgments

This work is supported in part by the Grant-in-Aid for Scientific Research (grant no. 20048001) from the Ministry of Education, Culture, Sports, Science and Technology (MEXT), Japan. A part of this work was conducted in Kyoto-Advanced Nanotechnology Network, supported by 'Nanotechnology Network' of the MEXT, Japan.

### References

- [1] Bachtold A, Fuhrer M S, Plyasunov S, Forero M, Anderson E H, Zettl A and McEuen P L 2000 *Phys. Rev. Lett.* **84** 6082
- [2] Yao Z, Kane C L and Dekker C 2000 *Phys. Rev. Lett.* **84** 2936
- [3] Dresselhaus M, Dresselhaus G and Avouris Ph 2001 *Carbon Nanotubes: Synthesis, Structure, Properties and Applications* (Berlin: Springer)
- [4] Tsukagoshi K, Alphenaar B W and Ago H 1999 *Nature* **401** 572
- [5] Huang S, Woodson M, Smalley R and Liu J 2004 *Nano Lett.* **4** 1025
- [6] Tsukagoshi K and Alphenaar B W 2000 *Superlatt. Microstruct.* **27** 565
- [7] Inami N 2008 Characterization of carbon nanotube field effect transistor fabricated by direct synthesis method *PhD Thesis* Japan Advanced Institute of Science and Technology
- [8] Julliere M 1975 *Phys. Lett. A* **54** 225
- [9] Sahoo S, Kontos T, Furer J, Hoffmann C, Graber M, Cottet A and Schonenberger C 2005 *Nat. Phys.* **1** 99
- [10] Nagabhirava B, Bansal T, Sumanasekera G U and Alphenaar B W 2006 *Appl. Phys. Lett.* **88** 023503
- [11] Inami N, Mohamed M A, Shikoh E and Fujiwara A 2007 *Sci. Technol. Adv. Mater.* **8** 292
- [12] Sagnes M, Raquet B, Lassagne B, Broto J M, Flahaut E, Laurent C, Ondarcuhu T, Carcenac F and Vieu C 2003 *Chem. Phys. Lett.* **372** 733